The family of molecular conductors $[(n\text{-Bu})_4N]_2[M(dcbdt)_2]_5$, M = Cu, Ni, Au; band filling and stacking modulation effects†

Elsa B. Lopes,[a] Helena Alves,[a] Isabel C. Santos,[a] David Graf,[b] James S. Brooks,[b] Enric Canadell[c] and Manuel Almeida*[a]

Received 19th December 2007, Accepted 2nd April 2008
First published as an Advance Article on the web 24th April 2008
DOI: 10.1039/b719418h

Single crystals of the partially oxidised complexes $[(n\text{-Bu})_4N]_2[M(dcbdt)_2]_5$ with M = Au, Ni and Cu (dcbdt = 4,5-dicyanobenzene-1,2-dithiolate) have been obtained by electrocrystallisation techniques. These compounds are isomorphous and present a triclinic structure, space group $P\bar{1}$. Their crystal structures were solved for the Au compound at 120 K and 298 K and for Ni compound at 120 K and consist of pentamerised segregated stacks of the partially oxidised complex along [−2,1,0], arranged in layers alternating with cation layers. Their physical properties (electrical conductivity and thermopower) are compared and related on the basis of extended Hückel calculations to the different electronic bandfillings imposed by the different metals and their slightly different structures. The lower electrical conductivity, $\sigma_{RT} = 0.15$ S cm^{-1}, with a larger activation energy, $E_a = 176$ meV, as well as the larger magnitude of thermopower of the Ni compound, are consequences of both a more pronounced modulation of the stacking and electronic bandfilling with a Fermi level at a distortion induced gap. Both Au and Cu compounds present higher conductivity values, $\sigma_{RT} = 10$ S cm^{-1}, with very small activation energy (27 and 16 meV respectively) and in the Au compound a clear metallic regime is induced down to 100 K under a pressure of 9 kbar.

Introduction

The field of molecular conductors has experienced a significant development particularly after the discovery of superconductivity in the Bechgaard salts. The vast majority of molecular conductors and superconductors that have been reported so far are based on TTF derivatives. The transition metal bisdithiolene complexes, which can be seen as inorganic analogs of TTF with the metal replacing the central C=C bond of TTF, as building blocks for conducting materials, have been however comparatively less explored. These transition metal bisdithiolene complexes have frontier orbitals identical to the corresponding TTFs with the additional possibility that depending on the transition metal group and oxidation state they can bear different magnetic moments, thus being more versatile building blocks for molecular materials.

In spite of the fact that recently it has been found that some of these bisdithiolene complexes can present high electrical conductivity and metallic properties in their neutral state (the so called single component molecular metals)[1] the established strategy to obtain high electrical conductivity relies on the preparation of partially oxidised salts which even with simple ligands can give molecular metals such as $Li_{0.7}Pt(mnt)_2$[2] and with sulfur rich ligands such as dmit can even lead to superconductivity.[3] Therefore there is great interest in further exploring the possibility of using other dithiolene ligands to obtain conducting materials based on inorganic transition metal complexes

We recently described a new series of transition metal bisdithiolene complexes based on the aromatic extended ligand dcbdt (4,5-dicyanobenzene-1,2-dithiolate), $M(dcbdt)_2$ (Scheme 1), with different transition metals M = Ni, Cu, Au, Pd, Pt, Fe and Co,[4] which have started to be used as building blocks for conducting and magnetic materials.[5] One of the characteristics of these complexes is that, as a consequence of the relatively large and extended π-system of the ligand, they are easily oxidised and preliminary data indicating large electrical conductivity in the partially oxidised compounds $[(n\text{-Bu})_4N]_2[M(dcbdt)_2]_5$ with M = Au and Ni, have already been reported.[4a,6] However previously the low quality and small size of the crystals have limited the structural analysis and other studies of these compounds.

In this paper we report a comprehensive characterisation of this family of partially oxidized complexes, including the new Cu analogue, a full structural analysis of the Ni and Au compounds based on accurate refinements and theoretical calculations which are used to discuss the differences in their physical properties.

The comparison of the Ni compound with the Cu and Au analogues provides a clear example of the effect of bandfilling

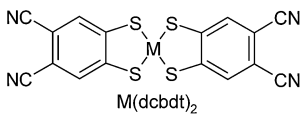

Scheme 1

[a]*Depart. Química, ITN / CFMCUL, P-2686-953 Sacavém, Portugal. E-mail: malmeida@itn.pt; Fax: +351 219550117; Tel: +351 219946171*
[b]*NHMFL/Physics, Florida State University, Tallahassee, Florida 32310, USA. E-mail: brooks@magnet.fsu.edu; Fax: +1 8506445038; Tel: +1 8506442836*
[c]*Institut de Ciència de Materials de Barcelona, (CSIC), E-08193 Bellaterra, Spain. E-mail: canadell@icmab.es; Fax: +34 935805729; Tel: +34 935801853*

† CCDC reference numbers 670913–670915. For crystallographic data in CIF or other electronic format see DOI: 10.1039/b719418h

variation on the physical properties of molecular conductors without any change in stoichiometry or counterion structural modification.

Experimental

Synthesis

Dichloromethane was distilled over phosphorus pentoxide under argon atmosphere. $(n\text{-Bu})_4N[M(dcbdt)_2]$ with M = Ni, Au and Cu were prepared as previously described.[4a,c] Other chemicals were commercially obtained and used without any further purification. $[(n\text{-Bu})_4N]_2[Cu(dcbdt)_2]_5$ with M = Ni, Cu and Au were prepared by electrocrystallisation using the same general conditions previously described for M = Ni.[4]

$[(n\text{-Bu})_4N]_2[Cu(dcbdt)_2]_5$. A procedure similar to that previously described for the M = Ni analogue was followed.[4] A dry and deaerated solution of $(n\text{-Bu})_4N[Cu(dcbdt)_2]$ (30 mg, 4.4×10^{-2} mmol) in dichloromethane (20 ml) was placed under argon atmosphere in a electrocrystallisation cell with two compartments separated by fritted glass and with platinum electrodes. After about 7 days under galvanostatic conditions, ~1.5 μA cm^{-2}, dark green thin needles, with a metallic shine, formed over the anode (up to $\sim 2 \times 0.05 \times 0.02$ mm^3) were collected and washed with cold dichloromethane. Mp >350 °C; elemental analysis calcd (%) for $C_{112}H_{92}N_{22}S_{20}Cu_5$ (2705.04): C 49.73, H 3.43, N 11.39, S 23.70; found: C 50.02, H 3.24, N 11.27, S 23.19.

$[(n\text{-Bu})_4N]_2[Au(dcbdt)_2]_5$. $[(n\text{-Bu})_4N]_2[Au(dcbdt)_2]_5$ was prepared from $(n\text{-Bu})_4N[Au(dcbdt)_2]$ following a similar procedure as for the Cu analogue. Single crystals of $[(n\text{-Bu})_4N]_2[Au(dcbdt)_2]_5$ as dark brown thin needles (up to $\sim 4 \times 0.1 \times 0.05$ mm^3) were obtained after ~10 days of electrocrystallisation. Mp >350 °C; elemental analysis calcd (%) for $C_{112}H_{92}Au_5N_{22}S_{20}$ (3372.14): C 39.89, H 2.75, N 9.14, S 19.01; found: C 40.25, H 2.54, N 9.09, S 19.41.

Crystallography

Room temperature X-ray diffraction data were collected on an Enraf-Nonius CAD4 diffractometer and low temperature (120 K) data on a Bruker AXS APEX CCD area detector diffractometer[7] equipped with an Oxford Cryosystems low-temperature platform, both using graphite monochromated Mo Kα radiation ($\lambda = 0.71073$Å). For CAD4 data at room temperature absorption corrections were applied semi-empirically using Psi-Scan,[8] while for CCD at low temperature they were applied empirically using SADABS.[9] The structures were solved by direct methods using SIR97[10] and refined by full matrix least-squares methods with the SHELXL97[11] program using the winGX software package.[12] Non-hydrogen atoms were refined with anisotropic thermal parameters whereas H atoms were placed in idealized positions and allowed to refine riding on the parent C atom.

For the Ni compound and the Au compound at room temperature the poorer quality of the crystals resulted in a low percentage (about 40 and 36 respectively) of observed data [$I > 2\sigma(I)$]. As a consequence, several (66 and 200) restraints on displacement parameters (isor) had to be used for a satisfactory refinement with all non-H atoms refined with anisotropic displacement parameters. Although the structure determination of the Au compound at room temperature cannot be considered of high quality, the overall geometry of the complexes, which is of interest for the present discussion, is unambiguously determined as confirmed by the high quality low temperature resolution. Molecular graphics were prepared using ORTEP3[13] and SCHAKAL-97.[14]

Table 1 summarizes the details of crystallographic data collection and structure refinement. Selected bond lengths and bond angles are given in Table 2.†

Table 1 Crystallographic data for $[(n\text{-Bu}_4)N]_2[M(dcbdt)_2]_5$ compounds

	$(n\text{-Bu}_4N)_2[Ni(dcbdt)_2]_5$ (**1**)	$(n\text{-Bu}_4N)_2[Au(dcbdt)_2]_5$ (**2**)	$(n\text{-Bu}_4N)_2[Au(dcbdt)_2]_5$ (**3**)
T/K	120(2)	295(2)	120(2)
Formula	$C_{112}H_{92}Ni_5N_{22}S_{20}$	$C_{112}H_{92}Au_5N_{22}S_{20}$	$C_{112}H_{92}Au_5N_{22}S_{20}$
FW	2680.83	3372.11	3372.11
Cryst. Syst., Sp. Group	Triclinic, $P\bar{1}$	Triclinic, $P\bar{1}$	Triclinic, $P\bar{1}$
a/Å	7.9605(5)	7.973(4)	7.9351(1)
b/Å	17.0682(13)	17.322(3)	17.0822(3)
c/Å	22.3270(17)	23.1771(4)	22.9746(4)
α/deg	69.628(4)	68.119(9)	68.763(2)
β/deg	89.239(4)	88.882(8)	88.809(1)
γ/deg	79.236(4)	78.409(9)	78.163(1)
V/Å^3	2789.4(3)	2903.6(16)	2836.08(9)
Z, D_{calc}/Mg m^{-3}	1, 1.596	1, 1.928	1, 1.974
Cryst. size/mm	$0.18 \times 0.08 \times 0.02$	$0.36 \times 0.1 \times 0.01$	$0.30 \times 0.10 \times 0.03$
μ/mm^{-1}	1.264	6.713	6.873
θ-range/deg	2.60 to 25. 38	1.85 to 24.98	2.62 to 25.68
Index range, hkl	−9/9, −20/20, −26/26	−9/0, −20/20, −27/27	−9/9, −20/20, −28/28
Reflns collected	19519	11007	70525
Refl. unique [R(int)]	10020 [0.1179]	10206 [0.0871]	10747 [0.0495]
Abs. corr.	Multiscan	Psi-scan	Multiscan
T_{max}, T_{min}	0.9752 and 0.8044	0.943 and 0.462	0.8204, 0.2323
Refls $I > 2\sigma(I)$/Refin. par.	10020/722	10206/722	10747/722
S (on F^2)	0.882	0.885	1.005
$R_1(F)$, $wR(F^2)$, $I > 2\sigma(I)$	0.0726, 0.1229	0.0801, 0.0987	0.0245, 0.0529
$\Delta\rho$/e A^{-3}	+0.857, −0.6446	+1.428, −1.709	+0.958, −0.865

Table 2 Selected bond lengths for $[(n\text{-}Bu_4)N]_2[M(dcbdt)_2]_5$ compounds

	M = Ni 120 K	M = Au 298 K	M = Au 120 K
M(1)–S(1)	2.131(2)	2.297(8)	2.3018(9)
M(1)–S(1)[a]	2.131(2)	2.297(8)	2.3018(9)
M(1)–S(2)	2.127(3)	2.309(8)	2.3027(10)
M(1)–S(2)[a]	2.127(3)	2.309(8)	2.3027(10)
M(2)–S(3)	2.145(3)	2.320(9)	2.3009(10)
M(2)–S(4)	2.141(3)	2.297(8)	2.3068(10)
M(2)–S(5)	2.114(3)	2.303(8)	2.3026(10)
M(2)–S(6)	2.152(3)	2.329(8)	2.3062(9)
M(3)–S(7)	2.184(3)	2.278(8)	2.2999(9)
M(3)–S(8)	2.185(3)	2.271(8)	2.2965(10)
M(3)–S(9)	2.189(3)	2.295(8)	2.3045(9)
M(3)–S(10)	2.192(3)	2.259(8)	2.2959(9)
M(3)–S(7)[b]	2.402(2)		
M(3)–M(3)	3.016(2)		
S(1)–C(1)	1.687(10)	1.71(3)	1.740(4)
S(2)–C(2)	1.724(9)	1.67(3)	1.736(4)
S(3)–C(9)	1.693(10)	1.73(3)	1.738(4)
S(4)–C(10)	1.756(9)	1.75(2)	1.745(4)
S(5)–C(17)	1.709(9)	1.77(3)	1.734(4)
S(6)–C(18)	1.716(9)	1.71(3)	1.734(4)
S(7)–C(25)	1.769(9)	1.74(2)	1.747(4)
S(8)–C(26)	1.718(9)	1.73(3)	1.739(4)
S(9)–C(33)	1.751(9)	1.74(2)	1.731(4)
S(10)–C(34)	1.713(9)	1.78(3)	1.740(4)

[a] $-x+1, -y+2, -z+1$. [b] $-x+1, -y+1, -z+1$.

Theoretical calculations

The tight-binding band structure calculations were of the extended Hückel type.[15] A modified Wolfsberg–Helmholtz formula was used to calculate the non-diagonal $H_{\mu\nu}$ values.[16] The basis set consisted of Slater-type orbitals of double-ζ quality for Au 5d and of single-ζ quality for Au 6s and 6p, C 2s and 2p, S 3s and 3p, N 2s and 2p and H 1s. The ionization potentials, contraction coefficients for the double-ζ type orbitals and exponents were taken from previous work.[17]

Electrical transport mesurements

The electrical transport measurements were performed along the long axis of the needle shaped crystals, [−2,1,0]. Electrical resistivity and thermopower at ambient pressure were measured, as a function of temperature, using the same cell attached to the cold stage of a closed cycle helium refrigerator. In a first step thermopower was measured using a slow AC (10^{-2} Hz) technique by attaching to the extremities of the needle shaped crystals with platinum paint (Demetron 308A) two $\phi = 25$ μm 99.99% pure Au wires (Goodfellow Metals) anchored to two quartz thermal reservoirs, in a previously described apparatus,[18] controlled by a computer.[19] The oscillating thermal gradient was kept below 1 K, and it was measured with a differential Au–0.05 at.% Fe *versus* chromel thermocouple. The sample temperature was measured by a previously calibrated thermocouple of the same type. Both the differential thermocouple and the sample voltage were measured with Keithley 181 nanovoltmeters. The absolute thermopower of the sample was obtained after correction for the absolute thermopower of the Au leads, using the data of Huebner.[20] In a second step, electrical resistivity measurements were performed in the same sample using a four-probe technique. Without removing the crystal from the sample holder, two extra Au wires were placed on the sample in order to achieve a four-in-line contact configuration. Prior to the measurements the sample was checked for unnested to nested voltage ratio, as defined by Schafer *et al.*,[21] that was below 5%. Measurements were done imposing through the sample a current of 1 μA at low frequency (77 Hz) and measuring the voltage drop with a lock-in amplifier.

Resistivity measurements under pressure were done in a conventional BeCu clamp-type cell with Daphne oil as the pressure transmitting medium. The sample was glued with graphite paste to $\phi = 20$ μm diameter gold wires to make the electrical contacts. The pressures in the clamp cell were corrected to account for the pressure loss upon cooling.[22]

Results and discussion

Synthesis and characterisation

The $[(n\text{-}Bu)_4N]_2[M(dcbdt)_2]_5$ compounds with M = Ni, Cu and Au were obtained as small crystals under identical electrocrystallisation conditions. For M = Ni and Au the crystals were larger and of better quality, particularly for M = Au, enabling in addition to electrical measurements a full crystal structure analysis by X-ray diffraction. For M = Cu, probably as a consequence of a lower stability of the solutions, the crystals were more difficult to grow and best results were obtained with shorter assays and using larger currents. The crystals obtained with M = Cu were of smaller dimensions, barely enough for electrical transport measurements, and with quality not suitable for a full structure determination by X-ray diffraction.

Crystal structure

The $[(n\text{-}Bu)_4N]_2[M(dcbdt)_2]_5$ salts with M = Ni and Au are isomorphous, crystallizing in triclinic, space group $P\bar{1}$, with comparable cell parameters. The small crystal dimensions and quality of the Cu analogue did not enable the X-ray diffraction structural refinement but indicated similar unit cell with parameters $a = 7.99$ Å, $b = 17.09$ Å, $c = 22.40$ Å, $\alpha = 69.75°$, $\beta = 89.44°$, $\gamma = 79.39°$, $V = 2816$ Å^3, indicating an isomorphous situation in agreement with the similar physical properties (see below).

The structures of the M = Au and Ni compounds both consist of segregated stacks of the metal bisdithiolene complexes along [−2,1,0], as shown in Fig. 1 for M = Au. The stacks of $M(dcbdt)_2$ units are closely packed in layers parallel to the *ab* plane, alternating with layers of $(n\text{-}Bu)_4N$ cations. Fig. 1 (a) and (c) compares the stacks of the Ni and Au compound.

The asymmetric unit contains one half $M(dcbdt)_2$ complex (labeled 1) with the metal in an inversion center, two $M(dcbdt)_2$ complexes (labeled 2 and 3) and one cation. Therefore the stacks, as shown in Fig. 1 comparing Au and Ni, compounds, are made of the repeating sequence of five metal bisdithiolene complexes ...,123321,123321,... with three types of overlapping modes as shown in Fig. 2 for the Ni and Au compounds. In spite of the isomorphous situation there are as shown in Fig. 1 and 2 significant differences in the stacking modulation of the anions and in their overlapping modes.

In the gold compound the metal complexes are all fairly planar (the rms atomic deviations from the average molecular plane are 0.06, 0.08 and 0.05 Å for anions 3, 2 and 1 respectively) and they

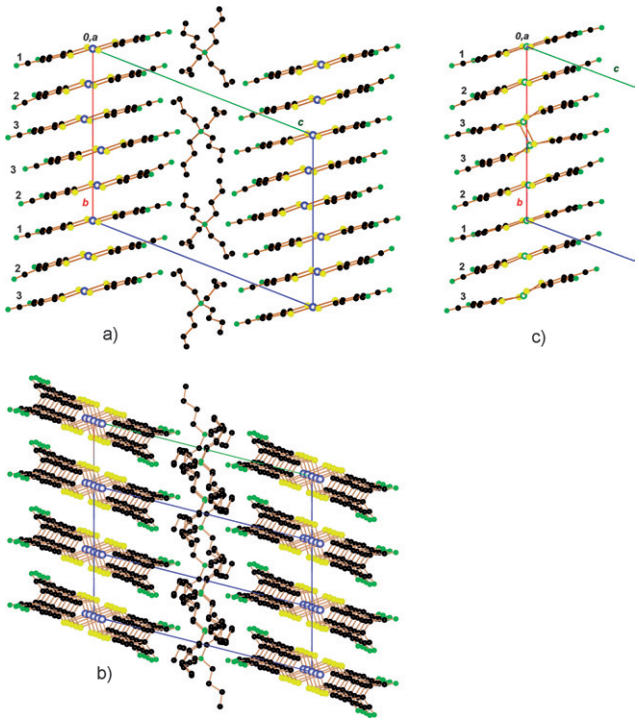

Fig. 1 Crystal structure of $[(n\text{Bu}_4)\text{N}]_2[\text{Au(dcbdt)}_2]_5$ viewed along *a* (a) and *b* − 2*a* (b), compared with a partial view of $[(n\text{Bu}_4)\text{N}]_2[\text{Ni(dcbdt)}_2]_5$ along *a* (c).

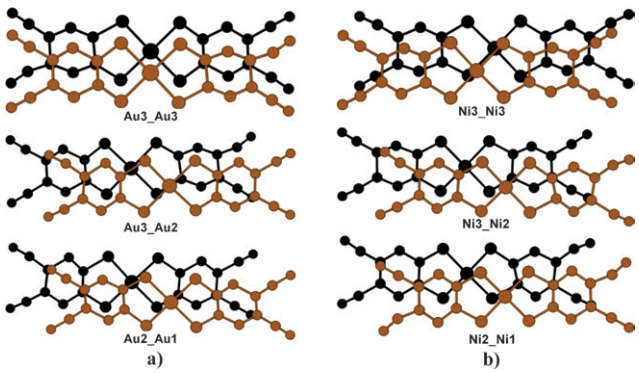

Fig. 2 The three different intrastack overlap modes in $[(n\text{Bu}_4)\text{N}]_2[\text{M(dcbdt)}_2]_5$, M = Au (left) and Ni (right).

are almost parallel to each other (the angles between average planes of complexes 1,2 2,3 and 3,3 are 3.70(5)°, 2.12(4)° and 0°, with comparable interplanar distances of 3.941(7) Å, 3.441(6) Å and 3.421(7) Å respectively.

Even within the reduced uncertainty of the structural refinement at 120 K the S–Au, S–C and C=C bond distances of the three different complexes are identical within experimental uncertainty (Table 2) indicating a partially oxidized situation where the two electrons responsible for the anionic component of this compound are equally delocalized among the five gold complexes of the unit cell.

In the Ni compound a much stronger modulation in the anionic stacking pattern is observed as shown in Fig. 1(c). While the Ni2 and Ni1 anions are almost planar (the rms atomic deviations from the average plane are 0.06 and 0.04 Å respectively) the Ni3 anion presents a distorted geometry and a Ni3–Ni3 overlap mode clearly distinct from the gold analogue. Here there are Ni–S apical bonds (2.402(2) Å) almost identical to those observed in the salt $(n\text{Bu}_4\text{N})_2[\text{Ni(dcbdt)}_2]_2$ (2.3965(16) Å) where the complexes are strongly dimerised.[4a] This suggests an almost complete localisation of the two extra electrons responsible for the anionic charge of the compound in the dimerised $[\text{Ni3(dcbdt)}_2]_2^{2-}$ units with the three other complexes being close to neutral. This picture is further supported by the analysis of Ni–S bond lengths which for Ni1 (2.130 Å) and Ni2 (2.144 Å) have average values significantly shorter than for Ni3 (2.188 Å) which in turn are close to those of $(n\text{Bu}_4\text{N})_2[\text{Ni(dcbdt)}_2]_2$ (2.196 Å).[4a]

Electrical transport properties

The electrical conductivity, σ, measured along the long axis of the needle shaped crystals of $[(n\text{-Bu}_4)\text{N}]_2[\text{Cu(dcbdt)}_2]_5$ is plotted as a function of the temperature in Fig. 3 together with those of the Ni[4a] and Au[6] analogues. At room temperature the conductivity was found to be ~10 S cm^{-1}, a value comparable to that previously found for the Au analogue. Its temperature dependence shows an activated behaviour with a rather small activation energy of 16 meV, slightly smaller than that found for the Au analogue (Fig. 3).[6] In the Au compound there is a small decrease of activation energy around 80 K, from 27 to 12 meV, that is not observed in the Cu samples. This may be attributed to a change from an intrinsic to an extrinsic regime. Due to the very small size of the crystals and high resistance of contacts, the Cu compound could not be measured below 40 K. The electrical conductivities of the Au and Cu compounds are therefore comparable and at least two orders of magnitude larger than that of the Ni compound which also shows a much larger activation energy of 176 meV at higher temperatures.

The thermoelectric power measurements (Fig. 4) also show comparable results for Au and Cu compounds, quite different from the Ni analogue. The thermopower of the Cu compound is 4 μV K^{-1} at room temperature, only slightly different from that

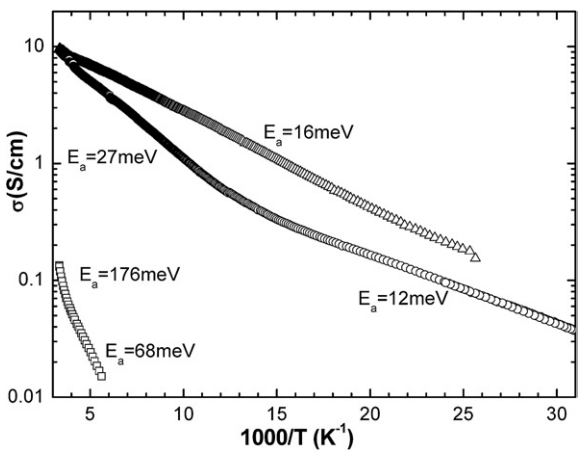

Fig. 3 Electrical conductivity, σ, of $[(n\text{-Bu}_4)\text{N}]_2[\text{M(dcbdt)}_2]_5$ single crystals as a function of the inverse temperature; M = Cu (△), Au (○),[4] Ni (□).[4a]

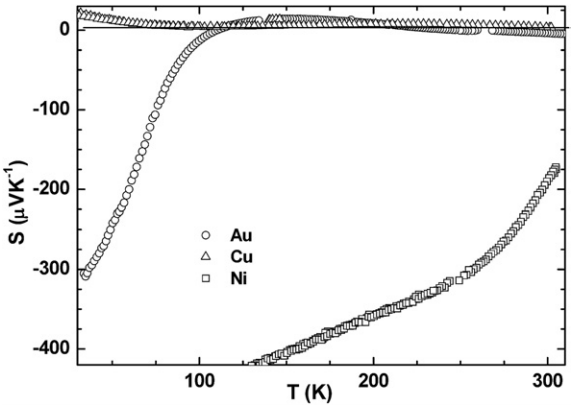

Fig. 4 Absolute thermopower, S, of $[(n\text{-}Bu_4)N]_2[M(dcbdt)_2]_5$ single crystals as a function of temperature; M = Cu (△), Au (○),[4] Ni (□).[4a]

of the Au analogue (-6 μV K^{-1}), in both compounds with negligible temperature dependence down to 100 and 50 K for Au and Cu respectively. The thermopower of the Au compound below 100 K, approximately the temperature where the electrical conductivity activation energy decreases, starts dropping fast toward negative values, indicating a gap around the Fermi level and consistent with a change towards an extrinsic regime, while for Cu only a rather modest increase is observed below 50 K. The high temperature behaviour with rather small S values and negligible temperature dependent values, denotes a symmetry of transport above and below the Fermi level consistent with a half filled band system or with a small gap degenerated semiconductor. These results contrast with the Ni analogue which shows large negative and strongly temperature dependent thermopower values, denoting a clear semiconducting regime in agreement with the electrical conductivity.

Under pressure the electrical conductivity shows a significant increase, doubling its room temperature value at 9 kbar (Fig. 5) while the temperature dependence changes. At 7 kbar there is already at high temperatures a significant range with a metallic regime ($d\sigma/dT < 0$) that under 9 kbar extends down to 100 K. However at 9 kbar, the highest pressure tested, the resistivity at lower temperatures gradually becomes thermally activated and

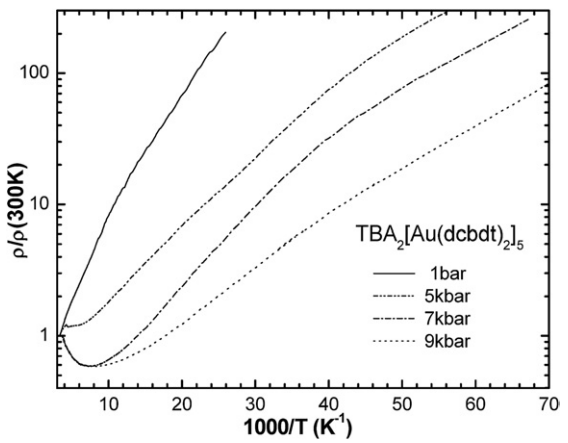

Fig. 5 Electrical resistivity, ρ, of $[(n\text{-}Bu_4)N]_2[Au(dcbdt)_2]_5$ as a function of the inverse temperature under different pressures indicated.

an activation energy of ~8 meV is observed below 50 K under 9 kbar. Since this change of regime is rather gradual and no maximum of the activation energy is observed it most probably reflects gradual localization effects due to correlation rather than a real metal to insulator transition.

Electronic band structure and general discussion

The different properties of the Ni, Cu and Au compounds are expected to reflect both structural differences in the stacking modulation of the complexes and the differences in the electronic band filling as previously pointed out on a qualitative basis.[6a] In order to better understand and access the role of each of these two contributions we performed electronic band structure calculations based on the above described crystal structure refinements of the Ni and Au compounds at different temperatures.

The electronic band structures were calculated considering the different intermolecular interactions between anions which are arranged in layers as schematically shown in Fig. 6. Here the three crystallographically non-equivalent transition metal complexes are engaged in nine different intermolecular interactions (I–IX). Three of them are intrastack interactions (I–III), three are lateral π-type interactions (V–VII), and three are σ-type interactions along step-chains (IV, VIII and IX). It was found more convenient for these calculations to use a repeat unit built from the a and $b' = (b - 2a)$ repeat vectors. This new unit cell has exactly the same area as that built from a and b but with the advantage that one of the repeat vectors, b', goes along the stacks direction.

In the gold compound the electronic structure near the Fermi level originates from the singly occupied molecular orbital (SOMO) of $Au(dcbdt)_2$, which is essentially the out-of-phase combination of a π-type orbital of the two dithiolene moieties which mixes in the Au d_{xz} orbital (see Fig. 7; this orbital corresponds to the LUMO of the $Ni(dcbdt)_2$ complex). The SOMO energies for the three gold complexes 1, 2 and 3 are quite similar, -11.46, -11.44 and -11.52 eV, respectively, so that although the three acceptors are structurally different from the electronic viewpoint, they can be considered as almost equivalent, in agreement with the almost identical bond lengths and geometry.

In order to gain some information about the strength of the SOMO···SOMO interactions, which are at the origin of the

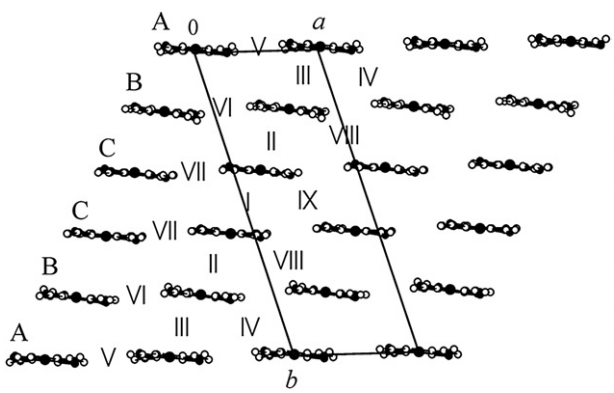

Fig. 6 Acceptor layer of $[(n\text{-}Bu_4)N]_2[Au(dcbdt)_2]_5$ viewed along c where the different intermolecular interactions are labelled.

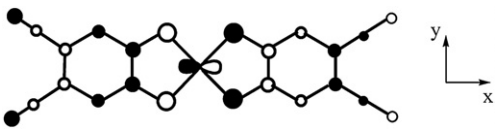

Fig. 7 Schematic representation of the SOMO of $Au(dcbdt)_2$.

spread of the SOMO levels into bands, we have calculated the $\beta_{SOMO-SOMO}$ interaction energies, which are a useful measure of the interaction between the SOMO of a given $Au(dcbdt)_2$ and that of a nearest neighbor, for the nine different types of intermolecular interactions in the layer. The absolute values of these energies as well as the S···S contacts shorter than 3.9 Å associated with each interaction are reported in Table 3. Two observations can be made: 1) all interstack interactions are very small, at least one order of magnitude smaller than the intrastack interactions, and 2) the three intrastack interactions are large and quite similar. Consequently, since the three SOMO energies are similar it is expected that the $Au(dcbdt)_2$ layers behave as a series of very weakly interacting quasi-uniform chains.

Table 3 Absolute values of the $\beta_{HOMO-HOMO}$ intermolecular interaction energies (eV)[23] and S···S distances shorter than 3.9 Å for the different anion···anion interactions in $[(n\text{-}Bu)_4N]_2[Au(dcbdt)_2]_5$ at 120 K (298 K). The values in parentheses are for the room temperature structure

Interaction	S···S (<3.9 Å)	$\beta_{HOMO-HOMO}$/eV
I	3.683(×2), 3.684(×2) (3.737(×2), 3.743(×2))	0.3994 (0.3228)
II	3.774, 3.795 (3.830, 3.837)	0.3328 (0.2809)
III	3.820, 3.825 (3.847, 3.944)	0.2868 (0.2819)
IV	3.519, 3.739, 3.750 (3.568, 3.809, 3.814)	0.0260 (0.0230)
V	3.644 (3.670)	0.0037 (0.0051)
VI	3.669 (3.718)	0.0007 (0.0006)
VII	3.654 (3.679)	0.0028 (0.0027)
VIII	3.557, 3.769, 3.825 (3.602, 3.843, 3.863)	0.0246 (0.0217)
IX	3.479 (3.514)	0.0363 (0.0330)

The calculated band structure near the Fermi level is shown in Fig. 8. Since there are five transition metal complexes per repeat unit there are five bands almost exclusively built from the SOMO of $Au(dcbdt)_2$. The calculated band structure at 298 K completely agrees with the qualitative analysis previously made.[6] There are five bands strongly remembering a five-folded SOMO band along the $\Gamma \rightarrow Y$ direction (*i.e.* the b'^* direction) whereas the five bands are very flat along the $\Gamma \rightarrow X$ direction (*i.e.* the a^* direction). This is exactly what is expected for a layer built from weakly interacting and quite uniform chains with five $Au(dcbdt)_2$ units in the unit cell. It is quite remarkable that despite the presence of three different transition metal complexes and three different intermolecular modes, the $Au(dcbdt)_2$ chains behave as quasi-uniform as far the electronic structure is concerned.

The dashed line in Fig. 8 is the Fermi level calculated assuming a metallic filling of the bands, neglecting electronic repulsion effects. The associated Fermi surface, which is made of a series of almost non-warped lines perpendicular to the stacking direction, b, is shown in Fig. 9. However, in view of the relatively small bandwidths, the role of electron repulsion effects is expected to be relatively important and the validity of the band model may become questionable. Indeed the observed transport properties at ambient pressure indicate a thermally activated behaviour, although with small activation energy, rather than the clear metallic regime predicted by the band model. A metallic temperature dependence of resistivity is however recovered under pressure, presumably due to the increased bandwidth.

The band structure calculated based on the structure at 120 K (Fig. 8b) presents more than five bands because the lower SOMO

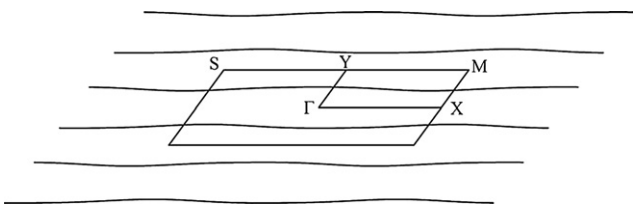

Fig. 9 Calculated Fermi surface for $[(n\text{-}Bu_4)N]_2[Au(dcbdt)_2]_5$ assuming a metallic filling of the bands.

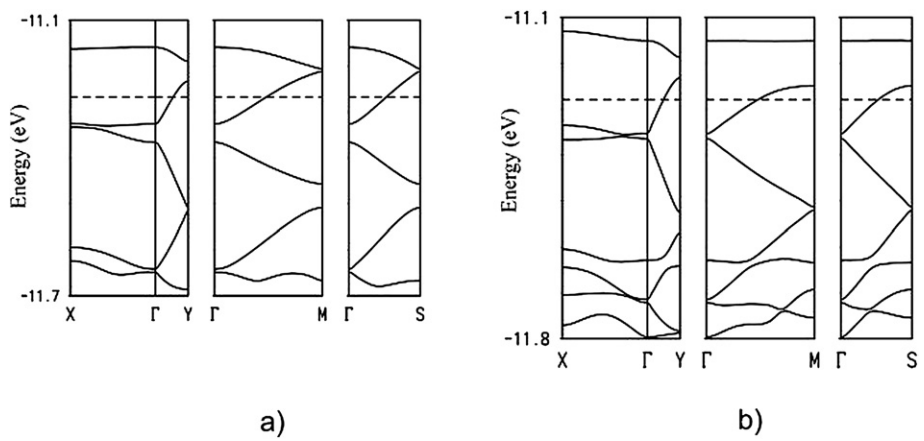

Fig. 8 Calculated band structures for the $Au(dcbdt)_2$ layer at 298 K (a) and 120 K (b). The dashed line is the calculated Fermi level assuming a metallic filling of the bands. $\Gamma = (0, 0)$, $X = (a^*/2, 0)$, $Y = (0, b'^*/2)$, $M = (a^*/2, b'^*/2)$ and $S = (-a^*/2, b'^*/2)$ where the repeat vectors are defined as $a' = a$ and $b' = (b - 2a)$.

bands slightly overlap with the next lower bands. For instance an avoided crossing along the chain direction implicating the second lower SOMO band can be noticed. The total width of the SOMO bands has increased approx. 16% mainly due to an increase of intrastack interactions I, II and III while the transverse interactions remain relatively weak. As a consequence the Fermi surface presents similar lines, just a little bit flatter than at 298 K.

The observed effect of pressure on electrical conductivity can be understood as a result of an even larger bandwidth increase, enough to stabilize a metallic regime at higher temperatures. The effect of hydrostatic pressure certainly will increase the intrastack interactions but the interstack ones can behave differently due to their sensitivity to minor changes in the tilting of molecules. A more quantitative analysis should wait for the results of the crystal structure analysis under pressure.

The results of the band structure for $[(n\text{-}Bu_4)N]_2[Ni(dcbdt)_2]_5$ at 120 K, calculated in a similar way, are shown in Fig. 10 where are shown ten bands around the Fermi level built from the HOMO and LUMO (the equivalent of the SOMO of $Au(dcbdt)_2$) of the $[Ni(dcbdt)_2]$ complex. The lower four bands are based on the HOMO of the acceptors. The next five bands are based on the LUMO of the acceptors and have the same shape as the five SOMO bands of the Au analogue. Finally, the upper band is exclusively made of the HOMO of the two complexes making the dimeric unit. The five LUMO bands are quite delocalized among the five complexes. The bands of Fig. 10 must be filled with twelve electrons so that the Fermi level lies in a clearly defined gap at variance with the Au analogue. This is in agreement with the large activated nature of the conductivity in the Ni compound.

The origin of this somewhat unusual band structure is the nature of the Ni3–Ni3 dimeric unit. As shown by the band structure in Fig. 10 it does not affect very much the LUMO$\cdots$LUMO interactions along the chain but has a strong effect on the HOMO$\cdots$HOMO interactions. The dimerization strongly raises one HOMO level localized in the dimeric unit which becomes empty. Thus in contrast with the usual acceptor character of the $Ni(dcbdt)_2$ complex, three of them in $(TBA)_2[Ni(dcbdt)_2]_5$ behave in the usual way (*i.e.* accepting electrons) whereas two of them behave abnormally (*i.e.* losing electrons).

Although the gold chains could be formally considered as half-filled band systems, the band structure of Fig. 8 suggests that it is best described as a 7/10 filled band system and thus, despite the strong one-dimensional nature, the driving force for a distortion opening some kind of gap at the Fermi level must be quite small. A detailed analysis of the electronic band structure of the copper compound waits for a structural determination, but based on an isomorphous situation an isoelectronic configuration, similar to the Au analog, is expected to occur, and taking into account the smaller size of the Cu atom compared to Au, shorter intrastack contacts and larger electronic interactions are expected to occur.

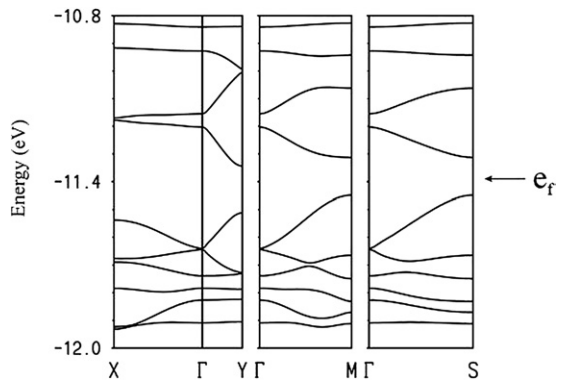

Fig. 10 Calculated band structure for $[(n\text{-}Bu_4)N]_2[Ni(dcbdt)_2]_5$ at 120 K. $\Gamma = (0, 0)$, $X = (a^*/2, 0)$, $Y = (0, b'^*/2)$, $M = (a^*/2, b'^*/2)$ and $S = (-a^*/2, b'^*/2)$, where the repeat vectors are defined as $a = a$ and $b' = (b - 2a)$.

Conclusions

In conclusion we have prepared and characterised three isomorphous compounds of a family of molecular conductors based on partially oxidised bisdithiolene complexes with different transition metals and variable properties ranging from small gap semiconductors to metallic under pressure. This family of compounds illustrates in clear way how a different band filling induced by different transition metals and the associated stacking distortions influence the physical properties of molecular conducting systems.

In spite of the very large number of molecule based conductors reported in the last 30 years of research, the band filling effects in molecular conductors have been difficult to probe experimentally. Since the vast majority of molecular conductors are charge transfer salts the band filling is essentially controlled by the counterion charge and stoichiometry. However the variation of any of these factors leads in most cases to drastic structural modifications. Even in cases where small stoichiometry variations could be made preserving the main pattern of the conducting network, the band filling variations cannot be isolated from changes in the counterion structure.[24] To the best of our knowledge, besides the recent study of $[Ni(dmdt)_2]$, $[Au(dmdt)_2]$ conductors based on a neutral species and their alloys,[1d,e] this is the first time that band filling effects are clearly put into evidence in molecular conducting salts, preserving the stoichiometry and without being associated with any counterion structural variation.

Acknowledgements

This work was partially supported by FCT (Portugal) under contract POCI/QUI/57528/2004, an FLAD/NSF grant, MEC (Spain) under Project FIS2006-12117-C04-01, Generalitat de Catalunya (2005 SGR 683), and NSF-DMR 0602859 (USA).

References

1 (*a*) D. Belo, H. Alves, E. B. Lopes, M. T. Duarte, V. Gama, R. T. Henriques, M. Almeida, A. Pérez-Benítez, C. Rovira and J. Veciana, *Chem.–Eur. J.*, 2001, **7**, 511; (*b*) H. Tanaka, Y. Okano, H. Kobayashi, W. Suzuki and A. Kobayashi, *Science*, 2001, **291**, 285; (*c*) A. Kobayashi, E. Fusjiwara and H. Kobayashi, *Chem. Rev.*, 2004, **104**, 5243–5264; (*d*) W. Suzuki, E. Fujiwara, A. Kobayashi, Y. Fujishiro, E. Nishibori, M. Takata, M. Sakata, H. Fujiwara and H. Kobayashi, *J. Am. Chem. Soc.*, 2003, **125**, 1486–1487; (*e*) B. Zhou, M. Shimamura, E. Fujiwara, A. Kobayashi, T. Higashi, E. Nishibori, M. Sakata, H. B. Cui, K. Takahashi and H. Kobayashi, *J. Am. Chem. Soc.*, 2006, **128**, 3872–3873; (*f*) J. P. M. Nunes, M. J. Figueira, D. Belo, I. C. Santos, B. Ribeiro, E. B. Lopes, R. T. Henriques, J. Vidal-Gancedo, J. Veciana, C. Rovira and M. Almeida, *Chem.–Eur. J.*, 2007, 9841–9849.

2 (*a*) M. Ahamad and A. E. Underhill, *J. Chem. Soc., Chem. Commun.*, 1981, 67; (*b*) M. Ahamad, D. J. Turner, A. E. Hunderhill, C. S. Jacobsen, K. Mortensen and K. Carneiro, *Phys. Rev. B*, 1984, **29**, 4796.
3 (*a*) P. Cassoux and L. Valade, in *Inorganic Materials*, 2nd edn, ed. D. W. Bruce and D. O'Hare, John Wiley and Sons, Chichester, 1996, p. 1; (*b*) P. Cassoux and J. S. Miller, in *Chemistry of Advanced Materials*, ed. L. V. Interrante and M. J. Hampden-Smith, Wiley-VCH, New York, 1998, p. 19.
4 (*a*) D. Simão, H. Alves, D. Belo, S. Rabaça, E. B. Lopes, I. C. Santos, V. Gama, M. T. Duarte, R. T. Henriques, H. Novais and M. Almeida, *Eur. J. Inorg. Chem.*, 2001, 3119–3126; (*b*) H. Alves, D. Simão, H. Novais, I. C. Santos, C. Giménez-Saiz, V. Gama, J. C. Waerenborgh, R. T. Henriques and M. Almeida, *Polyhedron*, 2003, **22**, 2481–2486; (*c*) H. Alves, D. Simão, I. C. Santos, V. Gama, R. T. Henriques, H. Novais and M. Almeida, *Eur. J. Inorg. Chem.*, 2004, 1318–1329.
5 (*a*) H. Alves, D. Simão, I. C. Santos, E. B. Lopes, H. Novais, R. T. Henriques and M. Almeida, *Synth. Met.*, 2003, **135–136**, 543–544; (*b*) D. de Caro, H. Alves, M. Almeida, S. Cailleux, M. El Gaddari, C. Faulmann, I. Malfant, F. Senocq, J. Fraxedas, A. Zwick and L. Valade, *J. Mater. Chem.*, 2004, **14**, 2801–2806.
6 (*a*) H. Alves, D. Simão, E. B. Lopes, D. Belo, V. Gama, M. T. Duarte, H. Novais, R. T. Henriques and M. Almeida, *Synth. Met.*, 2001, **120**, 1011; (*b*) H. Alves, I. C. Santos, E. B. Lopes, D. Belo, V. Gama, D. Simão, H. Novais, M. T. Duarte, R. T. Henriques and M. Almeida, *Synth. Met.*, 2003, **135–136**, 397–399.
7 Bruker. *SMART and SAINT*, Bruker AXS Inc., Madison, Wisconsin, USA, 2004.
8 A. C. T. North, D. C. Phillips and F. S. Mathews, *Acta Crystallogr., Sect. A*, 1968, **24**, 351–359.
9 G. M. Sheldrick, *SADABS*, Bruker AXS Inc., Madison, Wisconsin, USA, 2004.
10 A. Altomare, M. C. Burla, M. Camalli, G. Cascarano, G. Giacovazzo, A. Guagliardi, A. G. G. Moliterni, G. Polidori and R. Spagna, *J. Appl. Crystallogr.*, 1999, **32**, 115.
11 G. M. Sheldrick, *SHELXL97, Program for Crystal Structure Refinement*, University of Göttingen, Germany, 1997.
12 L. J. Ferrugia, *J. Appl. Crystallogr.*, 1999, **32**, 837.
13 L. J. Ferrugia, *J. Appl. Crystallogr.*, 1997, **30**, 565.
14 E. Keller, *SCHAKAL-97, A Computer Program for the Representation of Molecular and Crystallographic Models*, Kristallographisches Institut der universität Freiburg i.Br., Germany, 1997.
15 M.-H. Whangbo and R. Hoffmann, *J. Am. Chem. Soc.*, 1978, **100**, 6093.
16 J. H. Ammeter, H.-B. Bürgi, J. Thibeault and R. Hoffmann, *J. Am. Chem. Soc.*, 1978, **100**, 3686.
17 (*a*) A. J. Schultz, H. H. Wang, L. C. Soderholm, T. L. Sifter, J. M. Williams, K. Bechgaard and M.-H. Whangbo, *Inorg. Chem.*, 1987, **26**, 3757; (*b*) L. F. Veiros, M. J. Calhorda and E. Canadell, *Inorg. Chem.*, 1994, **33**, 4290.
18 M. Almeida, S. Oostra and L. Alcácer, *Phys. Rev. B*, 1984, **30**, 2839.
19 E. B. Lopes, INETI-Sacavém, internal report, 1991.
20 R. P. Huebner, *Phys. Rev. A*, 1964, **135**, 1281.
21 D. E. Schafer, F. Wudl, G. A. Thomas, J. P. Ferraris and D. O. Cowan, *Solid State Commun.*, 1974, **14**, 347.
22 K. Murata, H. Yoshino, H. O. Yadav, Y. Honda and N. Shirakawa, *Rev. Sci. Instrum.*, 1997, **68**, 2490.
23 (*a*) M.-H. Whangbo, J. M. Williams, P. C. W. Leung, M. A. Beno, T. J. Emge and H. H. Wang, *Inorg. Chem.*, 1985, **24**, 3500; (*b*) since overlap is explicitly included in extended Hückel calculations, these interaction energies (β) should not be confused with the conventional transfer integrals (t). Although the two quantities are obviously related and have the same physical meaning, the absolute values of β are somewhat larger than those of t.
24 M. Almeida, M. G. Kanatzidis, L. M. Tonge, T. J. Marks, H. O. Marcy, W. J. McCarthy and C. R. Kannewurf, *Solid State Commun.*, 1987, **63**, 457–461.

